The Astrophysical Journal, 642:1173–1176, 2006 May 10

RELATIONSHIP BETWEEN SOLAR WIND AND CORONAL HEATING: SCALING LAWS FROM SOLAR X-RAYS

N. A. Schwadron[1,2]
Department of Astronomy, Boston University, 725 Commonwealth Avenue, Boston, MA 02215; and Southwest Research Institute, P.O. Drawer 28510, San Antonio, TX 78228-0510; nathanas@bu.edu

and

D. J. McComas and C. DeForest
Southwest Research Institute, P.O. Drawer 28510, San Antonio, TX 78228-0510; dmccomas@swri.edu, deforest@boulder.swri.edu
Received 2005 June 13; accepted 2006 January 6

ABSTRACT

Pevtsov et al. recently showed that the luminosity of solar and stellar X-rays from closed magnetic structures scales nearly linearly with magnetic flux over 12 decades. We show here that the total power available to accelerate the solar wind also scales linearly with magnetic flux, provided that its sources inject a roughly constant energy per particle prior to losses from heat conducted by electrons into radiation. Using a recently developed model of the solar wind energy source and particle source, we calculate the available solar wind power and convert it into an equivalent X-ray luminosity to explore whether the same process that drives solar wind may also power coronal heating. The quantitative results agree remarkably well with the Pevtsov et al. X-ray observations and with *GOES* X-ray observations over almost two solar cycles from 1985 to 2004. The model for the solar wind energy and particle source relies on the continual reconfiguration of the supergranular network through the emergence of small bipolar or more complex closed magnetic fields. This naturally leads to an energy flux proportional to field strength on large-scale field structures with field strengths larger than the emerging flux. We conclude that the sources of energy for the solar wind and coronal heating are linked, likely through the emergence of new magnetic flux that continually reconfigures large-scale solar magnetic fields and powers and heats the corona.

Subject headings: solar wind — Sun: corona — Sun: X-rays, gamma rays

Online material: color figure

1. INTRODUCTION

The speed of the solar wind observed in situ in interplanetary space at 1 AU and beyond is strongly anticorrelated with its coronal freezing-in temperature (Geiss et al. 1995, Fig. 2; von Steiger et al. 2000, Fig. 6), which is determined from the charge state distributions of heavy elements. The freezing-in temperature is set where the solar wind draws ions out faster than they can equilibrate (through ionization and recombination) to the local electron temperature. Schwadron & McComas (2003) suggested that this anticorrelation between solar wind speed and freezing-in temperature results naturally if both fast and slow solar winds arise from the same small-scale structures that inject a roughly fixed electromagnetic energy per particle, $m\bar{v}_a^2$, but that a slow solar wind radiates more energy due to higher coronal temperatures. The roughly fixed injected electromagnetic energy per particle leads naturally to a well-organized final solar wind speed. In regions where conductive and radiative losses are insignificant, the final wind speed achieves its maximum steady state value of $\sim$800 km s^{-1},

$$\frac{mu_{\max}^2}{2} = m\bar{v}_a^2 - \frac{GM_s m}{R_s}, \tag{1}$$

and the coronal source temperature is cool, as observed in coronal holes. This expression (eq. [1]) was derived by Fisk et al. (1999) by relating magnetohydrodynamic Poynting and particle flux to the emergence of new magnetic flux on the Sun. In contrast, a slow wind is formed from hotter and brighter regions, where heat conduction funnels more energy into radiative loss near the base of the transition region (Schwadron & McComas 2003).

The concept that different types of solar wind originate from small-scale magnetic source structures that inject a roughly fixed energy per particle begs a deeper question: Do these same principles apply more generally to the closed corona, and possibly to other magnetic stars? We begin to address this question here. We use solar X-ray observations as a proxy for the heating processes that occur in the closed corona as a whole, and we directly compare the power that heats the corona to that which generates the solar wind. In § 2, we discuss the relationship between the Pevtsov et al. (2003) scaling law for X-rays and the solar wind. In § 3, we discuss this relationship in the evolution of X-rays over the solar cycle, and we provide concluding remarks in § 4.

2. FROM SOLAR WIND TO X-RAYS

Here we relate solar wind observations to observed X-ray luminosities. We start by deriving the power required to drive the solar wind and then relate this to the expected power in the X-ray spectral window. The parameterizations introduced by Schwadron & McComas (2003) require an energy flux, $\bar{Q}_0$, from small-scale structures that is given by

$$\bar{Q}_0 = \left(\frac{mu_{\max}^2}{2} + \frac{GM_s m}{R_s}\right) f_0, \tag{2}$$

[1] Also at: Center for Space Physics, Boston University, 725 Commonwealth Avenue, Boston, MA 02215.
[2] Also at: Center for Integrated Space Weather Modeling, Boston University, 725 Commonwealth Avenue, Boston, MA 02215.

where f_0 is the base particle flux. Because, on average, both the particle and magnetic flux are roughly constant at 1 AU (McComas et al. 2000), the average base flux is proportional to the average base field strength B_0 such that $f/B_r = f_0/B_0 = f_1/B_{1r} =$ constant (f and B_r are the particle and radial magnetic field at any position along the flux tube, the subscript "0" denotes the base fluxes near the Sun, and the subscript "1" denotes fluxes at 1 AU). We assume that small-scale emerging structures that power the solar wind inject a roughly constant energy per particle. Accordingly, the value of $u_{\max}$ is constant. In addition, the quantities f_1 and B_{1r} are observed to be constant. The resulting injected energy flux is then proportional to the base magnetic field strength. By integrating the base energy flux (eq. [2]) over the cross-sectional area of a flux tube, we derive an expression for the total power, $P_{\rm sw}$, that is available to drive the solar wind:

$$P_{\rm sw} = \left(\frac{mu_{\max}^2}{2} + \frac{GM_s m}{R_s}\right)\frac{f_1}{B_{1r}}\Phi_0, \qquad (3)$$

where Φ_0 is the base magnetic field flux of the open magnetic field that carries a steady fast solar wind.

Using $u_{\max} = 800$ km s^{-1}, $f_1 = 2\times10^8$ cm^{-2} s^{-1}, and $B_{1r} = 30$ μG, which are all from measured solar winds (McComas et al. 2000), we find $P_{\rm sw} \sim 50{,}000\Phi_0$, as shown by the solid line in Figure 1. Although the magnitude of the solar wind power is higher than the X-ray luminosity, the slopes are similar, and both are linearly proportional to magnetic flux.

Consider the situation in which the same process that powers the solar wind also heats the corona. In that case, the maximum power available to accelerate the solar wind should be the same as that available to heat the corona, provided that the magnetic flux is also the same. Whereas on open field lines injected energy and matter form a solar wind, on closed structures, the energy must be entirely converted into radiation:

$$mf_0 v_{a0}^2 = C_0\frac{\kappa_0 T_m^{7/2}}{L}, \qquad (4)$$

where T_m is the temperature maximum at or below a scale height, L is the length along a magnetic loop to this temperature, the coefficient of electron heat conduction is $\kappa_0 \approx 10^{-6}$ K$^{-7/2}$ ergs cm^{-1} s^{-1} (Spitzer 1962), and the dimensionless constant C_0 is found to be $C_0 \sim 0.91$ (Schwadron & McComas 2003). On the right-hand side of equation (4), we estimate the peak conductive flux using the maximum temperature and the loop length. It is well known from coronal loop models that this conductive flux estimate also provides a good ballpark estimate for the flux of energy radiated by the semiloop (Rosner et al. 1978). X-rays are formed from the energy conducted down the loops by electrons and provide a measure of the total radiative losses.

In the observed spectral window of *Yohkoh* soft X-rays (2.8–36.6 Å), the radiation is $\alpha_{\rm Yok} \sim 1\%$ of the power deposited in the corona (Longcope 2004). We recovered this fraction using the differential emission measure (DEM) distributions for the quiet Sun, active regions, and coronal holes that were provided with the CHIANTI software package (Dere et al. 1997; Young et al. 2004). These DEM distributions use solar atmospheric profiles of temperature and density from Vernazza & Reeves (1978) and simulated spectra for an average coronal hole, an average quiet Sun, and an average active region. Coronal abundances are from Feldman et al. (1992), and we have taken a constant pressure of 3×10^{15} cm^{-3} K. From the simulated spectra, we took the ratio, $\alpha_{\rm Yok}$, of power in the 2.8–36.6 Å band (integrated over the instrument response) over the power in the 1–940 Å band. We set an upper limit of 940 Å to exclude all emissions except hydrogenic lines emitted by the partially ionized plasma at the base of the transition region. We found $\alpha_{\rm Yok} = 0.8\%$ in active regions and $\alpha_{\rm Yok} = 0.5\%$ in quiet regions.

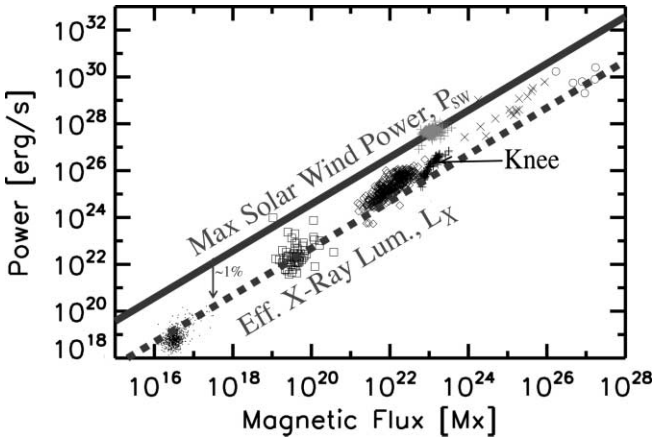

FIG. 1.—Model X-ray luminosity (*dashed line*) scaled from the maximum power available to accelerate the solar wind (Schwadron & McComas 2003; *solid line*), showing remarkable agreement with the X-ray luminosity over 12 decades. The black data points from Pevtsov et al. (2003) cover an enormous range of closed structures on the Sun and other stars, including the quiet sun (*dots*), X-ray–bright points (*squares*), solar active regions (*diamonds*), solar disk averages (*plus signs*), G, K, and M dwarfs (*crosses*), and T Tauri stars (*circles*). The light gray data points are from 1 day–averaged *Ulysses* observations of the fast solar wind over the mission life (to date). To derive the magnetic flux and total power, we multiply the 1 day–averaged power density and magnetic flux density by an area factor, $4\pi R_{\rm Uly}^2$, where $R_{\rm Uly}$ is *Ulysses*'s radial position. The agreement shown in this figure suggests that coronal heating and solar wind acceleration are powered by a similar source. [*See the electronic edition of the Journal for a color version of this figure.*]

Following the scenario for a similar coronal and solar wind energy source, the X-ray luminosity ($L_{\rm X}$) from closed structures is $\alpha_{\rm Yok} \sim 1\%$ of the maximum solar wind power,

$$L_{\rm Yok} \approx \alpha_{\rm Yok} P_{\rm sw} = 500\Phi_0. \qquad (5)$$

The resultant luminosity (Fig. 1, *dashed line*) agrees remarkably well with the X-ray observations.

Although our power law was derived only on the basis of the solar wind, it scales with the luminosity over the large 12 decade range of magnetic flux. In addition, since temperatures should increase on average with magnetic flux, the slight variation at higher magnetic fluxes (Fig. 1, *crosses*; G, K, and M dwarfs) may be due to a better match at increased temperatures between the bulk of the radiated spectrum and the spectral window of these X-ray observations.

It is well known that the X-ray luminosity varies significantly over the solar cycle, whereas the magnetic flux and fast solar wind power are relatively constant over the solar cycle. This begs the question, if the sources of coronal heating and solar wind are similar, then why is the X-ray luminosity so much more variable over the solar cycle?

3. X-RAY LUMINOSITY OVER THE SOLAR CYCLE

We investigate the evolution of X-rays and magnetic flux over the solar cycle to address why the solar wind power and magnetic flux are so much more constant than the X-ray power. The data shown in the middle panel of Figure 2 are the X-ray luminosities in the 1–8 Å range measured by the *Geostationary Operational Environmental Satellite* (*GOES*) for each Carrington rotation

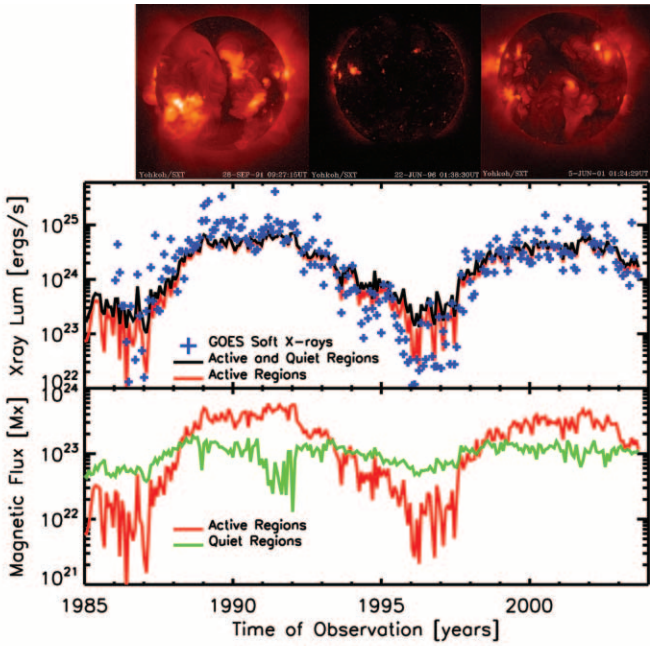

FIG. 2.—X-ray luminosity and magnetic flux in active and quiet regions over the solar cycle. The top images show *Yohkoh* soft X-ray images in 1991 September (*left*), 1996 June (*middle*), and 2001 June (*right*). The blue data points in the middle panel show soft X-ray luminosity (in units of ergs s^{-1}) from *GOES* (1–8 Å). The red and black curves in the middle panel show predictions that assume that the same power that generates the solar wind also heats the corona. The predictions are that $L_X = \alpha_{GOES} A_w \Phi_0$, where $A_w \approx 50{,}000$ is the conversion factor from magnetic flux into luminosity and α_{GOES} is the fraction of this power emitted in the 1–8 Å spectral window measured by *GOES* (we have also folded in the instrument response). In active regions, the spectral fraction is $\alpha_{GOES} \approx 2.3 \times 10^{-4}$; in quiet regions, $\alpha_{GOES} \approx 4.7 \times 10^{-5}$, and in coronal holes, $\alpha_{GOES} \approx 8 \times 10^{-10}$. In the middle panel, contributions of active regions (*red curve*) and combined active and quiet regions (*black curve*) are shown. In the bottom panel, we show the active region magnetic flux (*red curve*), approximated by all magnetic flux with field strength exceeding 60 G, and the portion of quiet region magnetic flux that is closed below 1.1 solar radii (*green curve*). The quiet region flux neglects small-scale mixed-polarity flux on scales less than $\sim 5^\circ$ (see text for details).

from 1985 to 2004. We have used *GOES* because the data are supplied over such a long time period. There is a 3 decade change in the X-ray luminosity from solar minimum to solar maximum, whereas the total solar magnetic flux changes by only an order of magnitude (Wang et al. 2000). We found that the X-ray luminosity is roughly proportional to the unsigned magnetic flux, cubed.

At least part of this variability in the X-rays is due to a change over the solar cycle in the fraction of the coronal emission in the 1–8 Å spectral window. We analyzed simulated radiated spectra emitted from active regions, quiet regions, and coronal holes (Dere et al. 1997; Young et al. 2003) and formed a ratio, α_{GOES}, of the power emitted in the 1–8 Å band (integrated over the instrument response) to the power emitted from 1 to 940 Å. The observed X-ray luminosity in the *GOES* 1–8 Å spectral window is the fraction α_{GOES} times the total power deposited into coronal heating, $L_{GOES} = \alpha_{GOES} P_{corona}$. In active regions, the spectral fraction is $\alpha_{GOES} \approx 2.3 \times 10^{-4}$; in quiet regions, $\alpha_{GOES} \approx 4.7 \times 10^{-5}$, and in coronal holes, $\alpha_{GOES} \approx 8 \times 10^{-10}$. We have used the same atmospheric profiles of temperature and density in active, quiet, and coronal hole regions, as previously discussed.

To make quantitative estimates of the X-ray flux over the solar cycle, we analyzed Kitt Peak Carrington maps and divided the magnetic flux into three bins: active region flux Φ_{AR}, quiet region flux Φ_{QR}, and open magnetic flux Φ_{CH}. As with the previous estimate in Figure 1, we take $P_{corona} \sim 50{,}000\Phi$, and we separate contributions to the luminosity according to the appropriate fluxes:

$$L_{GOES} = 50{,}000(\alpha_{AR}\Phi_{AR} + \alpha_{QR}\Phi_{QR}). \quad (6)$$

We neglect contributions from the open field, since α_{GOES} is extremely small in coronal holes and the injected power is predominantly channeled into solar wind acceleration. Unsigned magnetic flux with field strengths greater than 60 G is associated with active regions. We used a potential source surface model (PSSM) with an associated Legendre polynomial expansion up to $l = 20$ moments and a source surface at 2.5 solar radii to calculate the net unsigned open magnetic flux. For the quiet region flux, we used the PSSM to calculate the net unsigned flux associated with loops of heights less than 1.1 solar radii (70,000 km) and field strengths less than 60 G. This is a fairly restrictive definition of quiet region flux, which neglects large loops with heights roughly above $\sim$1 scale height in a 1 MK corona. Furthermore, the magnetic flux associated with small loops with scale lengths less than $\sim$30,000 km is implicitly neglected by the truncated polynomial expansion ($l \leq 20$). Even with this restrictive definition, however, Figure 2 shows that the contribution from the quiet region flux leads to an overestimate of the *GOES* X-ray flux during the quietest periods of solar minimum. Since small-scale magnetic flux tends to dominate during solar minimum, this result suggests that emerging small-scale magnetic fields are very dim X-ray emitters.

The lack of X-ray emission from small-scale magnetic loops may be the natural result of their cool temperatures. Loop heights are observed to be correlated with temperature. Smaller loops within supergranules are cooler, typically $<$800,000 K (Feldman et al. 1999, 2005), than the larger loops extending above the network. The cooler the loops, the smaller the fraction of energy emitted in the 1–8 Å range of *GOES* X-rays. So even if the power emitted in the network was linearly proportional to magnetic flux, the resulting X-ray emissions would still be dim compared to emissions from hotter regions. Our main conclusion is that the large variability in X-ray flux over the solar cycle is the combined result of two complementary effects: (1) during active periods, the Sun is populated with a greater number of active regions, which have stronger magnetic fields and therefore emit more X-rays, and (2) active regions are also hotter and therefore emit more energy in the X-ray spectral window. Together, these effects lead to very large variability (by 3 orders of magnitude over the solar cycle).

In contrast to the highly variable X-ray power over the solar cycle, the fast solar wind power and magnetic flux are extremely constant. The constancy of the open magnetic flux is a reflection of its conservation (Fisk & Schwadron 2001) and the relative constancy of the Sun's dipole field (Wang et al. 2000). In contrast, the Sun's strong magnetic fields in active regions are highly variable over the solar cycle. This, combined with the higher temperatures in active regions, produces strong variations in X-rays: near solar maximum, the strong flux and high temperatures from active regions produce a large X-ray luminosity; near solar minimum, the paucity of active regions leads to a much lower X-ray flux. Therefore, the different solar cycle evolution of the solar wind and coronal X-rays does not contradict the argument that they are powered by similar sources. The favorable comparison between predictions and observations in Figure 2 supports the hypothesis of a common source. Although the total power scales with magnetic flux, the X-ray power exhibits greater variability than does the magnetic flux due to an intrinsic temperature dependence of X-ray sources. Strong flux concentrations typically

associated with active regions are typically hot and produce a larger fraction of the total radiated energy in X-ray bands.

4. CONCLUSIONS AND IMPLICATIONS

There are three major conclusions that we can draw on the basis of the results discussed here:

1. As a complete solar and Sun-like stellar ensemble, X-ray emitters (disk averages, active regions, quiet regions, X-ray–bright points, G, K, M dwarfs, and T Tauri stars) exhibit a global scaling law in which power is roughly proportional to magnetic flux (Pevtsov et al. 2003).
2. Subsets of the complete ensemble, such as disk averages, may exhibit departures from the global scaling law. For example, disk averages appear to be biased toward *strong* active region flux. This steeper power versus flux dependence may be the result of an additional temperature dependence of the X-ray power. Regions of higher magnetic flux, such as active regions, are often hotter and have a larger fraction of the total power emitted in the X-ray bands.
3. A recent model that provides an explanation for the observed anticorrelation between solar wind speed and coronal freezing-in temperatures (associated with carbon and oxygen charge states; Schwadron & McComas 2003) yields an injected power proportional to the base open magnetic field flux, consistent with the Pevtsov et al. (2003) scaling law. The model also relies on a roughly constant energy per particle injected by source structures. This model helps to explain the solar wind's strong organization around speed, the stability of the fast wind, the more variable slow wind, and the stronger enhancements of low first ionization potential ions observed in the slow wind.

In summary, we have made a connection between coronal heating and solar wind acceleration. As a complete solar and Sun-like stellar ensemble, X-ray emitters exhibit a global scaling law in which power is roughly proportional to magnetic flux (Pevtsov et al. 2003). A recent model that provides an explanation for the observed anticorrelation between solar wind speed and coronal freezing-in temperatures (associated with carbon and oxygen charge states; Schwadron & McComas 2003) yields injected power proportional to the base open magnetic field flux, consistent with the Pevtsov et al. (2003) scaling law. This suggests a fundamental similarity between the energy sources of coronal heating and solar wind acceleration. If the injected power that drives these processes results from reconfiguration of the supergranular network and the emergence of new magnetic flux, then the net power transmitted onto strong large-scale flux tubes should be proportional to their magnetic flux. This provides a likely explanation for the linear scaling of coronal and solar wind power with the magnetic flux of large-scale fields. We conclude that solar wind acceleration and coronal heating have a similar energy source, which is likely the emergence of new small-scale flux that causes the continual reconfiguration of the supergranular network.

We thank Dana Longcope and Len Fisk for useful discussions and Yohei Yamauchi for aiding with Kitt Peak data reduction. This work was supported by NASA's *Ulysses* program. N. A. S. was supported in part by the Center for Integrated Space Weather Modeling (CISM), which is funded by the STC Program of the National Science Foundation under agreement ATM-0120950 and by a NASA solar wind theory grant, NAG5-12780.

REFERENCES

Dere, K. P., Landi, E., Mason, H. E., Monsignori Fossi, B. C., & Young, P. R. 1997, A&AS, 125, 149
Feldman, U., Doschek, G. A., Schühle, U., & Wilhelm, K. 1999, ApJ, 518, 500
Feldman, U., Landi, E., & Schwadron, N. A. 2005, J. Geophys. Res., 110, 07109
Feldman, U., Mandelbaum, P., Seely, J. F., Doschek, G. A., & Gursky, H. 1992, ApJS, 81, 387
Fisk, L. A., & Schwadron, N. A. 2001, ApJ, 560, 425
Fisk, L. A., Schwadron, N. A., & Zurbuchen, T. H. 1999, J. Geophys. Res., 104, 19765
Geiss, J., et al. 1995, Science, 268, 1033
Longcope, D. 2004, in Proc. *SOHO* 15 Workshop, Coronal Heating, ed. J. Ireland, R. Walsh, D. Danesy, & B. Fleck (ESA SP-575; Paris: ESA), 198
McComas, D. J., et al. 2000, J. Geophys. Res., 105, 10419
Pevtsov, A. A., Fisher, G. H., Acton, L. W., Longcope, D. W., Johns-Krull, C. M., Kankelborg, C. C., & Metcalf, T. R. 2003, ApJ, 598, 1387
Rosner, R., Tucker, W. H., & Vaiana, G. S. 1978, ApJ, 220, 643
Schwadron, N. A., & McComas, D. J. 2003, ApJ, 599, 1395
Spitzer, L. 1962, Physics of Fully Ionized Gases (2nd ed.; New York: Interscience)
Vernazza, J. E., & Reeves, E. M. 1978, ApJS, 37, 485
von Steiger, R., et al. 2000, J. Geophys. Res., 105, 27217
Wang, Y.-M., Lean, J., & Sheeley, N. R., Jr. 2000, Geophys. Res. Lett., 27, 505
Young, D. T., et al. 2004, Icarus, 167, 80
Young, P. R., Del Zanna, G., Landi, E., Dere, K. P., Mason, H. E., & Landini, M. 2003, ApJS, 144, 135